

1 **High throughput functional variant screens via in-vivo production**

2 **of single-stranded DNA**

3 Max G. Schubert^{1,6,7*}, Daniel B. Goodman^{2,7}, Timothy M. Wannier¹, Divjot Kaur³, Fahim
4 Farzadfar⁴, Timothy K. Lu⁴, Seth L. Shipman^{2,5}, George M. Church^{1,4,6}

5 **Abstract:**

6 Tremendous genetic variation exists in nature, but our ability to create and characterize
7 individual genetic variants remains far more limited in scale. Likewise, engineering proteins and
8 phenotypes requires the introduction of synthetic variants, but design of variants outpaces
9 experimental measurement of variant effect. Here, we optimize efficient and continuous
10 generation of precise genomic edits in *Escherichia coli*, via in-vivo production of single-stranded
11 DNA by the targeted reverse-transcription activity of retrons. Greater than 90% editing
12 efficiency can be obtained using this method, enabling multiplexed applications. We introduce
13 Retron Library Recombineering (RLR), a system for high-throughput screens of variants,
14 wherein the association of introduced edits with their retron elements enables a targeted deep
15 sequencing phenotypic output. We use RLR for pooled, quantitative phenotyping of synthesized
16 variants, characterizing antibiotic resistance alleles. We also perform RLR using sheared
17 genomic DNA of an evolved bacterium, experimentally querying millions of sequences for
18 antibiotic resistance variants. In doing so, we demonstrate that RLR is uniquely suited to utilize
19 non-designed sources of variation. Pooled experiments using ssDNA produced in vivo thus
20 present new avenues for exploring variation, both designed and not, across the entire genome.

21

22 **Introduction:**

23 Constructing genotypes of interest and observing their effect on phenotype critically aids
24 our understanding of genetics and genome function. As methods for editing genomes have
25 progressed, this “reverse genetics” approach has expanded in breadth and scale, from knockout
26 libraries¹ to refactored genomes^{2,3}. These experiments can now be performed within multiplexed
27 pools, which allow an ever greater number of mutations to be explored across varied conditions.
28 Critically, both creating genotypes and observing phenotype within pools has necessitated

¹Harvard University, Boston, MA, USA; ²University of California, San Francisco, San Francisco, CA, USA; ³University of Warwick, United Kingdom; ⁴Massachusetts Institute of Technology, Cambridge, MA; ⁵Gladstone Institutes, San Francisco, CA, USA; ⁶Wyss Institute for Biologically Inspired Engineering, Harvard University, Boston, MA; ⁷These authors contributed equally: Max G. Schubert, Daniel B. Goodman; *email: mgschubert@gmail.com

29 development of new techniques. Transposon insertions⁴, marked integrations⁵ and CRISPR-
30 inhibition^{6,7} can create thousands of variants simultaneously within pooled experiments, and
31 targeted sequencing of these elements enables pooled measurement of variant phenotypes. These
32 advancements in experimental scale have fundamentally transformed our understanding of
33 genome function⁸.

34 However, these current high-throughput genetic techniques remain limited, in that they
35 typically introduce, ablate, or regulate kilobases of DNA to create variation. This contrasts with
36 point mutations, which are ubiquitous in natural variation⁹, and are indispensable for engineering
37 proteins¹⁰ and metabolic pathways¹¹. While modifying kilobases of DNA can add and subtract
38 functional elements such as genes and regulatory sequences from the genome, point mutations
39 can alter the function of these elements, accessing a larger phenotypic landscape.

40 Point mutations and other precision edits can be performed by oligonucleotide
41 recombineering, which creates precise genomic changes in many bacteria without incorporating
42 selective markers or other large DNA sequences^{12,13} (Fig 1B). This technique enables multiple
43 variants to be created simultaneously within pools¹⁴, but provides no means for determining the
44 phenotypes of these mutations within pools. Therefore, genome-wide recombineering requires
45 individual mutant clones to be isolated, genotyped, and phenotyped for causality to be
46 established, severely limiting throughput.

47 We reasoned that it would be possible to transform recombineering into a method for
48 pooled, genome-wide phenotypic measurement of large populations of precise genetic variants
49 using bacterial retroelements known as retrons. Retrons are poorly-understood prokaryotic
50 retroelements that undergo targeted reverse-transcription, producing single-stranded multi-copy
51 Satellite DNA (msDNA)^{15,16,17}. Previous work has shown that msDNA can function as a
52 recombineering donor, creating specific edits in the genome^{16,17}. This is accomplished by altering
53 the retron sequence to produce single-stranded DNA containing a mutation of interest
54 surrounded by homology to a targeted genomic locus (Fig 1A, 1C). Retron recombineering was
55 used for genome modification in response to a stimulus, as a form of memory¹⁷, but editing rates
56 far lower than canonical recombineering using electroporated DNA^{14,18} made it impractical for
57 studying mutants of physiological interest.

58 Here we explored the factors which limit retron recombineering, and demonstrate
59 significant improvements to its efficiency. We introduce Retron Library Recombineering (RLR),

60 wherein a plasmid-encoded retron element creates specified mutations at high frequencies and
61 remains in the cell to quantify mutants within multiplexed selections and screens via targeted
62 sequencing (Fig 1D). Efficient editing and targeted amplicon sequencing of retron cassettes
63 allows pooled phenotypic measurement of mutations across disparate genomic locations,
64 including millions of retron cassettes blanketing the entire genome. We show that RLR is a
65 generalizable, precision tool for multiplexed, high-throughput reverse genetics experiments.
66

67 **Results and Discussion:**

68 **Genotypic changes improve retron recombineering**

69 Previous work has established that a recombineering donor can be introduced into the
70 retron-derived msDNA, resulting in editing of the target locus when a single-stranded annealing
71 protein (SSAP) such as Red β of Enterobacteria phage λ is co-expressed^{16,17} (Fig 1C), but at a
72 lower efficiency than when electroporated oligonucleotides are used as a donor. If retron
73 recombineering could be made much more efficient, most cells bearing a given retron plasmid
74 would contain the corresponding mutation. Thus, the retron cassette itself could serve as a
75 “barcode” to identify mutants within mixed pools, enabling pooled screens of precisely-created
76 mutant strains.

77 To measure editing, retron plasmids were constructed to confer drug resistance variants
78 within the essential genes *rpoB* and *gyrA*, and co-expressed with Red β (Methods). The fraction of
79 cells edited after growth and induction of this system in batch culture for approximately 20
80 generations was measured by deep-sequencing the targeted locus, and by plating efficiency on the
81 relevant antibiotic (Fig 2A, Fig S1C). Initially, less than ~0.1% of *E. coli* bearing the retron
82 recombineering system incorporated the desired mutation (Fig 2B), replicating previous results¹⁷.

83 We first sought to improve this editing by investigating mismatch repair, which is known
84 to interfere with oligonucleotide recombineering because the desired edit forms a genomic
85 mismatch as a repair intermediate^{12,19} (Fig 1B, S1A). Inactivating mismatch repair by disruption
86 of *mutS* improved the frequency of retron recombineering approximately 150-fold and 2-fold for
87 *gyrA* and *rpoB* donors, respectively (Fig 2B). This difference in effect is explained by the known
88 variation in sensitivity to mismatch repair among nucleotide mismatches¹³. Mismatch repair was
89 therefore inactivated in subsequent experiments.

90 Additionally, previous studies have demonstrated that inactivation of exonucleases
91 improves oligonucleotide recombineering by up to 3-fold^{20,21}, and this effect has been shown for
92 retrон recombineering as well^{22,23}. Inactivation of exonuclease genes *recJ* or *sbcB* (also known as
93 *xonA*) individually provided benefit, and inactivation of both together increased the fraction of
94 genomes edited during induction of retrон recombineering in batch growth by 131 and 201-fold
95 for the *gyrA* and *rpoB* donors, respectively (Fig 2B, S1C). We suspect that exonuclease
96 inactivation results in a more dramatic benefit for retron recombineering, because
97 recombineering donors are available continuously at low abundance, in contrast to canonical
98 oligonucleotide recombineering, where donors are available transiently at high abundance.

99 Because editing occurs continuously in this system, we then explored monitoring the rate
100 of editing over time, and whether prolonged editing produces a high fraction of edited cells.
101 During continuous growth and induction of retron recombineering at the *gyrA* locus in a
102 turbidostat, edited alleles accrued at a rate consistent with at least 5% editing per generation (Fig
103 2C, Fig S2). 73 hours of growth and induction across four replicate experiments resulted in
104 edited fractions as high as 99%, with a mean of 92% (Fig 2C, Fig S1D).

105

106 **Optimization of RLR co-factors**

107 We built a population genetics model simulating both editing and the abundance of edited
108 populations to determine the effect of editing efficiency in multiplexed experiments (Fig S2A).
109 We found that beneficial phenotypes like antibiotic resistance can be observed and quantified
110 accurately with modest editing efficiency, because edited alleles will rapidly out-compete their
111 non-edited counterparts once selection is applied (Fig S2C). Detrimental alleles, however,
112 require more potent editing to observe even lethal effects (Fig S2D). Detrimental phenotypes
113 also require persistent induction to be observed, whereas beneficial alleles can be observed after
114 an initial pulse of induction (Fig S2B).

115 These considerations led us to seek further improvements in editing rate by exploring
116 other SSAPs, the proteins required to catalyze recombineering by recruiting and annealing
117 ssDNA to the replication fork¹⁹. While Red β is the canonical SSAP used in *E. coli*, its distant
118 relative CspRecT was found to improve recombineering efficiency in *E. coli*²⁴. Replacing Red β
119 with CspRecT further increased the edited fraction observed in batch growth by nearly 3-fold to
120 more than 12-fold for *gyrA* and *rpoB* donors, respectively (Fig 2B, S3B). Notably, requirements

121 for inactivating mismatch repair and exonucleases are also somewhat relaxed when using
122 CspRecT (Fig S3A).

123 To characterize improved editing across a sample of sequences and genomic regions, we
124 altered TAG “amber” stop codons to TAA “ochre” variants, a target of intensive recombineering
125 to produce highly altered genomes²⁵. Altering 10 amber stop codons within essential genes by
126 induction as before resulted in edited fractions from 65% to 89% (Fig 2D), consistent with editing
127 rates in the range of 5-11% per generation (Fig 2E). The mean edited fraction across all loci
128 examined was 76% (Fig 2D), exceeding the highest efficiency editing achieved using
129 oligonucleotide recombineering, to our knowledge.

130 We also sought to remove the requirement for the mutagenic $\Delta mutS$ genotype for
131 efficient editing. When a dominant-negative $mutL$ allele¹³ ($+mutL^*$) is transiently expressed, the
132 observed editing is equivalent to that observed in a $\Delta mutS$ background. This both minimizes the
133 genotypic requirements in the parent strain and the duration of mutagenic mismatch-repair-
134 deficient growth required (Fig 2F).

135 In summary, retron recombineering in the $\Delta mutS \Delta recJ \Delta sbcB$ background is thousands-
136 fold improved over Wild Type, and can result in edited fractions greater than 90% with
137 continuous editing. These improvements enable the presence of a retron cassette to identify its
138 corresponding mutant strain within pooled experiments, and we proceeded to use this system for
139 pooled experiments characterizing antibiotic resistance alleles. In tandem, we developed further
140 improvements using the co-factors CspRecT and $MutL^*$. This system achieves higher editing
141 rates and functions in a non-mutagenic strain background, enabling more demanding applications
142 of RLR in the future.

143

144 **Generation of barcoded mutant pools and detection of phenotypes using RLR**

145 With efficient retron recombineering established, targeted sequencing of retron cassettes
146 can be used as a measure of a mutant’s abundance in a population, and therefore its phenotype
147 within a pooled assay (Fig 1D). Antibiotic resistance is a growth phenotype of clinical
148 importance, so we first sought to investigate antibiotic resistance mutations using RLR. We
149 constructed a retron library conferring known *E. coli* rifampicin resistance mutations, known
150 *Mycobacterium tuberculosis* rifampicin resistance mutations, and mutations affecting resistance

151 to other antibiotics, and Neutral, deleterious, and lethal control mutations (Fig 3A). Red β was
152 expressed from the plasmid as an SSAP.

153 $\Delta mutS \Delta recJ \Delta sbcB$ *E. coli* were transformed with this retron plasmid library, were
154 induced in batch growth to acquire the desired mutations, and plated on solid medium with
155 rifampicin. Sequencing retrons from these samples before and after selection correctly
156 identified known rifampicin resistance mutations²⁶ by enrichment, while resistance alleles to
157 unrelated drugs and other control alleles were depleted⁷⁻⁹ (Fig 3C).

158 Mutations observed in rifampicin-resistant *Mycobacterium tuberculosis*²⁷ did not confer
159 detectable resistance in *E. coli*, with the exception of alleles altering the H526 residue of RpoB
160 previously implicated in *E. coli* rifampicin resistance. This suggests some context-dependence of
161 rifampicin resistance mutations across differing *rpoB* sequences.

162 A range of enrichment values was observed across resistance alleles, reflecting variation
163 in the ability to grow under selection. Selection across rifampicin concentrations establishes
164 inhibition curves for mutants within the pool (Fig 3D). In this way, RLR enables high
165 throughput, pooled identification of antibiotic resistant alleles and facile characterization of their
166 relative effects across a range of conditions.

167

168 Quantitative pooled measurement of growth rate

169 Many phenotypes of interest produce small changes in fitness, rather than binary growth
170 phenotypes^{9,28}. Mutations producing small fitness improvements at low antibiotic concentrations
171 can lead to the development of high-level antibiotic resistance²⁹. To use RLR to quantify growth
172 rate of mutants, we thus used growth in sub-inhibitory rifampicin as a model phenotype.

173 The pooled, barcoded mutant library constructed previously by RLR was grown at a sub-
174 inhibitory concentration of rifampicin (5 μ g/mL), and samples were collected across multiple
175 time points. Relative abundance of plasmids remained stable during transformation and induction
176 of editing, but began to diverge once sub-inhibitory rifampicin was applied (Fig 4B). The degree
177 to which resistant mutants outpace neutral controls is a quantitative measure of growth rate
178 which correlates well to mutations when their growth is measured individually (Fig 4C, S4A).
179 RLR, therefore, provides a quantitative growth rate measurement for alleles within a pool that is
180 comparable to testing all mutants individually, but inherently more scalable.

181

182 **RLR detects causal variants by using libraries prepared from evolved genomic DNA**

183 Antibiotic resistance can evolve in the lab, producing strains with numerous mutations,
184 able to grow in thousands-fold more concentrated antibiotic than their ancestors³⁰. We reasoned
185 that RLR could be used to determine the causal mutations leading to resistance in such isolates
186 by using random fragments of their genomic DNA to construct an RLR library. Most fragments
187 containing a variant should be capable of editing because we found little effect of mutation
188 position within donor oligonucleotides (Fig S3C).

189 Genomic DNA from an *E. coli* strain highly resistant to the antibiotic Trimethoprim³⁰
190 (TMP) was acoustically sheared into fragments, ligated to custom adapter sequences, and used to
191 construct RLR libraries containing tens of millions of members in Retron plasmids expressing
192 Red β as an SSAP (Fig. 5A). Retron donors comprised sequences averaging approximately 100bp
193 in length, providing over 50-fold coverage of the genome in unique fragments (Fig 5B, S6A,
194 S6B), ensuring that variants present in the evolved genome are well-represented in the genomic
195 RLR library. This library was then introduced into a $\Delta mutS \Delta recJ \Delta sbcB$ strain.

196 Induction of RLR and selection with Trimethoprim dramatically increased the abundance
197 of some donors containing variants at the *folA* locus (Fig 4B, 4C), which encodes the protein
198 target of TMP³⁰. Within RLR donors mapping to this region, coverage of two SNPs are highly
199 enriched, indicating they individually increase TMP resistance (Fig. 4C). Multiple retron donor
200 sequences independently contribute to the enrichment of both alleles (Fig. 4C). The more highly-
201 enriched allele lies upstream of the *folA* CDS and likely increases it's transcription, a well-
202 described route to TMP resistance³¹. The other is known to increase the catalytic rate of *FolA*,
203 leading to TMP resistance³¹. A third SNP within *folA* is not enriched, suggesting little or no
204 effect individually at this concentration of TMP. Mutations at this third position are known to
205 interact with *folA* mutations at the active site, but not confer resistance on their own³². The
206 ability to individually measure mutational effect during the selection itself, especially for
207 mutations so near each other in the genome, distinguishes this method from existing techniques
208 like P1 transduction, which transfer up to ~100kb of contiguous variation, and require
209 subsequent sequencing of hits for interpretation³³.

210 To identify alleles outside the *folA* locus providing additional resistance, we performed a
211 subsequent transformation of the genomic library into a strain bearing all *folA* mutations.
212 Sequencing of retron plasmids following selection with increased TMP identified several

213 enriched variants (Fig. 4D), including variants within known resistance determinants such as the
214 marR regulator of the multi-antibiotic resistance operon³⁴. In this manner, causal alleles can be
215 determined repeatedly from evolved or environmentally derived pools of variation, in order to
216 deconvolute phenotypes requiring multiple mutations.

217

218 **Discussion:**

219 Here we show that retron recombineering is a flexible, generalizable tool for genome
220 editing, surpassing the editing rates achieved by other markerless editing tools like
221 oligonucleotide recombineering. Pooled, barcoded mutant libraries can be prepared in this way
222 and used for multiplexed characterization of natural and synthesized allelic variants, a process
223 we call RLR. RLR enables millions of experiments to be performed simultaneously, and
224 genome-wide insights to be gained.

225 RLR is an alternative to CRISPR-based methods which also perform pooled phenotypic
226 measurements of mutant sequences. These CRISPR-based methods create edits by using a guide
227 RNA to direct targeted breakage, and a plasmid-borne donor DNA to repair these breaks with the
228 desired sequence, with phenotypic tracking permitted by amplicon sequencing of these
229 components^{35–38}. RLR’s “donor only” nature builds upon these “Guide + Donor” methods in
230 several key ways. RLR eliminates the requirement for a minimum edited difference from the
231 reference sequence, including single-base pair changes, to be characterized without requiring
232 additional synonymous mutations being incorporated solely to ablate recognition by a guide^{35–37}.
233 RLR also overcomes the requirement for targeting a suitable protospacer-adjacent motif (PAM),
234 which reduces editing efficiency of CRISPR-based methods as the distance to a PAM
235 increases^{35–37}. Intriguingly, production of ssDNA using a retron appears to improve break-
236 dependent methods in *S. cerevisiae*³⁵ and *E. coli*³⁹.

237 That RLR does not require a “guide” element paired with an editing donor simplifies
238 RLR elements. In contrast to the two unique elements required for “guide + donor” strategies, or
239 the three required for efficient Prime editing⁴⁰, RLR’s sole requirement is one unique donor
240 sequence within the retron. This relaxed design constraint enables RLR using non-designed
241 variation. We demonstrate this using random fragments of evolved DNA as an input. We expect
242 that this approach will also enable use of random, degenerate variation introduced into templates,

243 which is of great interest for characterizing sequences in-depth, and creating synthetic evolution
244 systems⁴¹.

245 That CRISPR is not a required component of RLR also creates the possibility that RLR
246 could be combined with engineered selections/screens of which CRISPR is already a component.
247 In addition, Cas9 is toxic in many bacteria, even when nuclease-null forms are used^{42, 43}. Non-
248 toxic editing methods may enable new applications which may otherwise be hampered by
249 expression of deleterious components.

250 The continuous, replication-dependent nature of RLR over multiple generations makes it
251 distinct from break-dependent methods which occur as a discrete process. This feature facilitates
252 RLR's high efficiency, but may limit its utility in organisms where it is not practical or desirable
253 to undergo multiple generations during editing. Editing over multiple generations may confer
254 unique benefits however, such as the ability to extend editing periods for higher efficiency
255 editing, and ability to edit during selection regimes for directed evolution. Continuous editing is
256 best understood through a population genetics framework, and we offer a straightforward model
257 for simulating these processes.

258 We have shown that editing is functional and high-efficiency across a sample of donor
259 sequences, but more work remains to understand variation in editing, and further improve editing
260 rates. RLR could feasibly be applied in a combinatorial manner, characterizing groups of
261 mutations, and strategies remain to be developed in this area. It also remains unexplored whether
262 RLR can be applied to large deletions and insertions, and possibly facilitate other alterations
263 such as inversions, duplications, and rearrangements.

264 Here RLR measures beneficial growth and selective phenotypes, and we outline how
265 improvement of editing makes deleterious phenotypes accessible. Non-growth phenotypes could
266 also be made accessible to pooled measurement by fluorescent reporters⁴⁴, biosensors⁴⁵, single-
267 cell transcriptomics⁴⁶, and a myriad of other screens⁸. Likewise, given that recombineering is
268 possible in a range of organisms including Eukaryotes^{46,47}, and retrons occur across a range of
269 organisms¹⁶, RLR should not be limited to use in *E. coli*, and development of RLR in other
270 genetic systems is an exciting area of future research.

271

272 References:

273 1. Baba, T. et al. Construction of *Escherichia coli* K-12 in-frame, single-gene knockout

274 mutants: the Keio collection. *Mol. Syst. Biol.* 2, 2006.0008 (2006).

275 2. Richardson, S. M. et al. Design of a synthetic yeast genome. *Science* 355, 1040–1044
276 (2017).

277 3. Hutchison, C. A., 3rd et al. Design and synthesis of a minimal bacterial genome. *Science*
278 351, aad6253 (2016).

279 4. van Opijnen, T. & Camilli, A. Transposon insertion sequencing: a new tool for systems-
280 level analysis of microorganisms. *Nat. Rev. Microbiol.* 11, 435–442 (2013).

281 5. Warner, J. R., Reeder, P. J., Karimpour-Fard, A., Woodruff, L. B. A. & Gill, R. T. Rapid
282 profiling of a microbial genome using mixtures of barcoded oligonucleotides. *Nat.*
283 *Biotechnol.* 28, 856–862 (2010).

284 6. Gilbert, L. A. et al. Genome-Scale CRISPR-Mediated Control of Gene Repression and
285 Activation. *Cell* 159, 647–661 (2014).

286 7. Peters, J. M. et al. A Comprehensive, CRISPR-based Functional Analysis of Essential
287 Genes in Bacteria. *Cell* 165, 1493–1506 (2016).

288 8. Gray, A. N. et al. High-throughput bacterial functional genomics in the sequencing era.
289 *Curr. Opin. Microbiol.* 27, 86–95 (2015).

290 9. Tenaillon, O. et al. Tempo and mode of genome evolution in a 50,000-generation
291 experiment. doi:10.1101/036806.

292 10. Heim, R. & Tsien, R. Y. Engineering green fluorescent protein for improved brightness,
293 longer wavelengths and fluorescence resonance energy transfer. *Curr. Biol.* 6, 178–182
294 (1996).

295 11. Hong, K.-K. & Nielsen, J. Recovery of phenotypes obtained by adaptive evolution through
296 inverse metabolic engineering. *Appl. Environ. Microbiol.* 78, 7579–7586 (2012).

297 12. Costantino, N. & Court, D. L. Enhanced levels of lambda Red-mediated recombinants in
298 mismatch repair mutants. *Proc. Natl. Acad. Sci. U. S. A.* 100, 15748–15753 (2003).

299 13. Nyerges, Á. et al. A highly precise and portable genome engineering method allows
300 comparison of mutational effects across bacterial species. *Proc. Natl. Acad. Sci. U. S. A.*
301 113, 2502–2507 (2016).

302 14. Wang, H. H. et al. Programming cells by multiplex genome engineering and accelerated
303 evolution. *Nature* 460, 894–898 (2009).

304 15. Lampson, B. C., Inouye, M. & Inouye, S. Retrons, msDNA, and the bacterial genome.
305 *Cytogenet. Genome Res.* 110, 491–499 (2005).

306 16. Simon, A. J., Ellington, A. D. & Finkelstein, I. J. Retrons and their applications in genome
307 engineering. *Nucleic Acids Res.* (2019) doi:10.1093/nar/gkz865.

308 17. Farzadfar, F. & Lu, T. K. Synthetic biology. Genomically encoded analog memory with
309 precise in vivo DNA writing in living cell populations. *Science* 346, 1256272 (2014).

310 18. Lajoie, M. J., Gregg, C. J., Mosberg, J. A., Washington, G. C. & Church, G. M.
311 Manipulating replisome dynamics to enhance lambda Red-mediated multiplex genome
312 engineering. *Nucleic Acids Res.* 40, e170 (2012).

313 19. Mosberg, J. A., Lajoie, M. J. & Church, G. M. Lambda red recombineering in *Escherichia*
314 *coli* occurs through a fully single-stranded intermediate. *Genetics* 186, 791–799 (2010).

315 20. Sawitzke, J. A. et al. Probing cellular processes with oligo-mediated recombination and
316 using the knowledge gained to optimize recombineering. *J. Mol. Biol.* 407, 45–59 (2011).

317 21. Mosberg, J. A., Gregg, C. J., Lajoie, M. J., Wang, H. H. & Church, G. M. Improving
318 Lambda Red Genome Engineering in *Escherichia coli* via Rational Removal of Endogenous
319 Nucleases. *PLoS ONE* vol. 7 e44638 (2012).

320 22. Simon, A. J., Morrow, B. R. & Ellington, A. D. Retroelement-Based Genome Editing and
321 Evolution. *ACS Synth. Biol.* 7, 2600–2611 (2018).

322 23. Farzadfar, F., Gharaei, N., Citorik, R. J. & Lu, T. K. Efficient Retroelement-Mediated
323 DNA Writing in Bacteria. doi:10.1101/2020.02.21.958983.

324 24. Wannier, T. M. et al. Improved bacterial recombineering by parallelized protein discovery.
325 doi:10.1101/2020.01.14.906594.

326 25. Lajoie, M. J. et al. Genomically recoded organisms expand biological functions. *Science* 342, 357–360 (2013).

328 26. Barrick, J. E., Kauth, M. R., Strelloff, C. C. & Lenski, R. E. *Escherichia coli rpoB* Mutants
329 Have Increased Evolvability in Proportion to Their Fitness Defects. *Molecular Biology and*
330 *Evolution* vol. 27 1338–1347 (2010).

331 27. Pozzi, G. et al. *rpoB* mutations in multidrug-resistant strains of *Mycobacterium tuberculosis*
332 isolated in Italy. *J. Clin. Microbiol.* 37, 1197–1199 (1999).

333 28. Tenaillon, O. et al. The Molecular Diversity of Adaptive Convergence. *Science* vol. 335
334 457–461 (2012).

335 29. Kepler, T. B. & Perelson, A. S. Drug concentration heterogeneity facilitates the evolution of
336 drug resistance. *Proc. Natl. Acad. Sci. U. S. A.* 95, 11514–11519 (1998).

337 30. Baym, M. et al. Spatiotemporal microbial evolution on antibiotic landscapes. *Science* 353,
338 1147–1151 (2016).

339 31. Tamer, Y. T. et al. High-Order Epistasis in Catalytic Power of Dihydrofolate Reductase
340 Gives Rise to a Rugged Fitness Landscape in the Presence of Trimethoprim Selection. *Mol.*
341 *Biol. Evol.* 36, 1533–1550 (2019).

342 32. Dion, A., Linn, C. E., Bradrick, T. D., Georghiou, S. & Howell, E. E. How do mutations at
343 phenylalanine-153 and isoleucine-155 partially suppress the effects of the aspartate-27-->serine
344 mutation in *Escherichia coli* dihydrofolate reductase? *Biochemistry* 32, 3479–3487
345 (1993).

346 33. Thomason, L. C., Costantino, N. & Court, D. L. *E. coli* genome manipulation by P1
347 transduction. *Curr. Protoc. Mol. Biol.* Chapter 1, Unit 1.17 (2007).

348 34. Sulavik, M. C., Gambino, L. F. & Miller, P. F. The MarR repressor of the multiple antibiotic
349 resistance (mar) operon in *Escherichia coli*: prototypic member of a family of bacterial
350 regulatory proteins involved in sensing phenolic compounds. *Molecular Medicine* 1, 436
351 (1995).

352 35. Sharon, E. et al. Functional Genetic Variants Revealed by Massively Parallel Precise
353 Genome Editing. *Cell* 175, 544–557.e16 (2018).

354 36. Garst, A. D. et al. Genome-wide mapping of mutations at single-nucleotide resolution for
355 protein, metabolic and genome engineering. *Nat. Biotechnol.* 35, 48–55 (2017).

356 37. Roy, K. R. et al. Multiplexed precision genome editing with trackable genomic barcodes in
357 yeast. *Nat. Biotechnol.* 36, 512–520 (2018).

358 38. Guo, X. et al. High-throughput creation and functional profiling of DNA sequence variant
359 libraries using CRISPR–Cas9 in yeast. *Nature Biotechnology* vol. 36 540–546 (2018).

360 39. Lim, H. et al. Multiplex generation, tracking, and functional screening of substitution
361 mutants using a CRISPR/retron system. doi:10.1101/2020.01.02.892679.

362 40. Anzalone, A. V. et al. Search-and-replace genome editing without double-strand breaks
363 or donor DNA. *Nature* vol. 576 149–157 (2019).

364 41. Simon, A. J., d’Oelsnitz, S. & Ellington, A. D. Synthetic evolution. *Nat. Biotechnol.* 37,
365 730–743 (2019).

366 42. Cho, S. et al. High-Level dCas9 Expression Induces Abnormal Cell Morphology in
367 *Escherichia coli*. *ACS Synth. Biol.* 7, 1085–1094 (2018).

368 43. Rock, J. M. et al. Programmable transcriptional repression in mycobacteria using an
369 orthogonal CRISPR interference platform. *Nat Microbiol* 2, 16274 (2017).

370 44. Kosuri, S. et al. Composability of regulatory sequences controlling transcription and
371 translation in *Escherichia coli*. *Proc. Natl. Acad. Sci. U. S. A.* 110, 14024–14029 (2013).

372 45. Rogers, J. K. et al. Synthetic biosensors for precise gene control and real-time monitoring of
373 metabolites. *Nucleic Acids Res.* 43, 7648–7660 (2015).

374 46. Dixit, A. et al. Perturb-Seq: Dissecting Molecular Circuits with Scalable Single-Cell RNA
375 Profiling of Pooled Genetic Screens. *Cell* 167, 1853–1866.e17 (2016).

376 47. Murphy, K. C. λ Recombination and Recombineering. *EcoSal Plus* vol. 7 (2016).

377 48. Barbieri, E. M., Muir, P., Akhuetie-Oni, B. O., Yellman, C. M. & Isaacs, F. J. Precise
378 Editing at DNA Replication Forks Enables Multiplex Genome Engineering in Eukaryotes.
379 *Cell* 171, 1453–1467.e13 (2017).

380

381

382 **Online Methods:**

383

384 **Preparation of Strains and plasmids**

385 Strain ECNR1 was modified to replace the bla ampicillin resistance cassette and the tetR
386 repressor at the lambda prophage locus with the tetA tetracycline resistance cassette, using
387 double-stranded recombineering as per Datsenko and Wanner¹. All strains were also modified by
388 inactivation of the araBAD operon using this method, conferring arabinose auxotrophy and
389 ensuring consistent induction with arabinose. Other genes were likewise inactivated where
390 relevant, and the antibiotic resistance markers removed using FLP recombinase as previously
391 described². Retron plasmid pFF745 (Addgene #61450) was a generous gift from Fahim
392 Farzadfar and Timothy Lu. New retror donor sequences were introduced by KLD mutagenesis
393 (New England Biolabs, NEB), or Gibson Assembly (NEB). Plasmids were modified to contain a
394 low-copy origin under stringent replication control (SC101) and a tightly-regulated promoter
395 (AraC-pBAD) to minimize variability in growth and plasmid titer among retror plasmid-bearing
396 populations(Fig S5), and enable tight repression of the editing system. Expression in this system
397 produced an effect on growth comparable to expressing GFP, an improvement on pFF745-
398 derived COLE1-pL_lacO expression systems which had larger impacts on growth(Fig S5). Beta
399 recombinase was replaced by CspRecT and mutL-E32K was added in relevant plasmids by

400 Gibson Assembly (NEB). See Supplemental Sequences for oligonucleotides used to perform
401 these alterations.

402

403 **Measurement of Editing**

404 To perform editing, strains were transformed with retrons via electroporation¹,
405 and plated to Lysogeny Broth (LB, Lennox formulation: 10g tryptone, 5g yeast extract, 5g
406 sodium chloride per 1 liter distilled, deionized water, or ddH₂O) with 25ug/mL
407 Chloramphenicol(LB-CM25) with 1.5% agar added. After 18-24 hours of growth at 34°C,
408 colonies were picked into 100uL of LB-CM25 in a 96-well plate and allowed to grow 6-8 hours,
409 reaching confluence. These un-induced pre-cultures were diluted 1000-fold into 1mL of LB-
410 CM25 containing 0.2% L-arabinose (LB-CM25ara) in a 96-well plate, and allowed to grow for
411 24 hours at 34°C with shaking at 900rpm, reaching confluence. This 1000-fold dilution and
412 growth was repeated once more for all cultures. Assuming density at confluence to be consistent,
413 the number of generations experienced with induction across both 1:1000 batch cultures is
414 approximately 20, because 2¹⁰ is equal to 1024. 120uL of these saturated cultures (OD₆₀₀
415 approximately 3.0) were sampled to measure editing via amplicon sequencing as described
416 below.

417 When growth in a turbidostat is indicated, strains were grown in an eVOLVER
418 instrument² (FynchBio). Turbidostat vials were maintained between OD₆₀₀ of 0.2 and 0.4, in LB-
419 CM25ara with 0.05% tween added to prevent biofilm formation, growing at 34 degrees with a
420 stir rate of 8. 1mL samples were sampled at the indicated time points to measure editing via
421 amplicon sequencing as described below.

422 To measure editing after batch growth, samples were centrifuged for 5 minutes at 4.8krcf,
423 the pellet resuspended in 10mM NaOH solution with 0.01% Triton-100, and incubated at 95°C
424 for 10 minutes in a thermocycler. The resulting lysates were centrifuged for 10 minutes at
425 4.8krcf at 4 degrees, and supernatants were stored at -20°C. PCR amplification of the genomic
426 region was performed in reactions containing 10uL Q5 2x Mastermix (NEB), 2uL lysate
427 supernatant, 0.2uL 50uM primer mixture for the locus (Supplemental sequences), 1uL Evagreen
428 dye (Biotium), and 6.8uL ddH₂O. Amplification was monitored in the SYBR channel on an
429 Eppendorf Realplex4 real-time PCR system until several cycles of productive amplification were

430 observed (typically less than 10 cycles), and the resulting amplicons were indexed for
431 sequencing as described below.

432

433 **Preparation of genome-derived retron plasmid libraries**

434 Trimethoprim-adapted strains s100 and s102 were a kind gift from Michael Baym⁴,
435 MG1655 was obtained from the Coli Genetic Stock Center (CGSC, Yale University), and
436 genomic DNA was isolated from 1.5mL LB cultures using the Promega Wizard Genomic DNA
437 purification kit (Promega), and quantified using the Qubit dsDNA HS reagent (Thermo Fisher).
438 4ug DNA was placed in a Covaris 520045 tube, and sheared for 1200 seconds in a Covaris M220
439 using 50W peak incident power, 20% duty factor, and 200 cycles per burst. Fragmented DNA
440 was visualized with a Bioanalyzer (Agilent), using a DNA 1000 chip (Agilent).

441 The resulting fragments were repaired, dA-tailed, and ligated to a custom adapter
442 sequence (see Supplemental sequences) using the NEBnext Ultra II DNA library prep kit for
443 Illumina (NEB). The resulting purified products were amplified in a reaction containing 25uL Q5
444 2x Mastermix (NEB), 2uL template, 0.5uL 50uM primer mixture (Supplemental sequences),
445 2.5uL Evagreen dye (Biotium), and 22.5uL ddH2O. Amplification was monitored in the SYBR
446 channel on an Eppendorf Realplex4 real-time PCR system until several cycles of productive
447 amplification were observed, typically less than 10 cycles, and were purified using DNA-binding
448 magnetic beads³.

449 Adapter-dimer fragments containing no ligated insert were removed by digestion with
450 BsaI enzyme and size-selective purification using DNA-binding magnetic beads³. After this
451 purification, adapter-dimer fragments were no longer detectable by gel-electrophoresis,
452 indicating their rarification in the pooled library.

453 A vector for Type-IIIs “Golden Gate” assembly was prepared via PCR, using a pBAD-
454 SC101 retron plasmid (with Beta or CspRecT, as indicated) as a template, and the resulting
455 amplicon was purified using DNA-binding magnetic beads³. Vector and insert were ligated
456 together in a Type-IIIs “Golden Gate” assembly, with restriction and ligation occurring in one
457 reaction mixture. This was performed in a reaction containing approximately .3pMol vector and
458 1pMol inserts, 2uL BsaI-v2, 2uL concentrated T4 DNA ligase (M202T, NEB). Reactions were
459 incubated for 5 minutes at 37degC, then for 30 cycles of 37degC and 20degC for 4 minutes each,
460 then finally for 60degC for 10 minutes, in a thermocycler.

461

462 **Preparation of Synthetic retrон plasmid libraries**

463 Recombineering donors were designed using the MODEST web tool⁴. Donors were
464 assembled from individual oligonucleotides (Integrated DNA Technologies) using Primerize⁵.
465 These donors were assembled into a compatible vector prepared by PCR (see supplemental
466 sequences).

467

468 **Introduction of plasmid libraries into strains, editing.**

469 Plasmid library assembly reactions were purified by Ethanol precipitation, eluted into
470 2uL of TE buffer, and chilled on ice. 50uL of thawed electrocompetent cells (Lucigen ELITE
471 10G) were introduced, and electroporated using the EC1 setting on a Bio-Rad MicroPulser. After
472 recovery in Lucigen Recovery medium for 1 hour at 37degC with shaking, 10mL of LB with
473 25ug/mL chloramphenicol was added for overnight growth at 30degC with shaking. Glycerol
474 stocks were prepared at this point, and plasmids were isolated by midi-prep(Qiagen).

475 Electrocompetent cells were prepared by growing 50mL of $\Delta mutS$, $\Delta recJ$, $\Delta sbcB$ in LB at
476 30degC until an OD₆₀₀ of 0.5 to 0.8 was achieved. These cultures were chilled on ice; pelleted,
477 resuspended, and rinsed twice with 50mL chilled 10% glycerol; then resuspended in 2mL chilled
478 glycerol for a final centrifugation. This pellet was resuspended in 150uL 10% glycerol, and 50uL
479 aliquots were used for electroporation and recovery as described above.

480 This recovery was washed with PBS, resuspended into LB and a 1/5 dilution of this
481 recovery was performed into 10mL LB-CM25Ara and grown for 6-8 hours at 34degC to saturate
482 the culture and dilute out non-transformed and/or dead cells from the recovery. Editing was
483 performed by diluting 1/1000 into 10mL(Synthetic libraries) or 50mL (genomic libraries) of LB-
484 CM25Ara and grown to saturation 34degC overnight. This process was repeated once more to
485 achieve greater than 20 generations of growth on average with induction.

486

487 **Binary Screens for drug resistance**

488 Barcoded Synthetic mutant libraries prepared as above were pelleted and rinsed with
489 PBS, before resuspending in PBS. Diluted samples were plated onto 100mm petri dishes
490 containing LB with relevant concentrations of rifampicin and 1ug/mL chloramphenicol, to
491 determine the CFU/ml plating efficiency across different conditions when grown overnight at

492 34degC. Not fewer than 6 petri dishes per condition were plated using a dilution targeting one
493 thousand colonies per plate, and grown overnight at 34degC. The resulting colonies were scraped
494 from the plates, rinsed and resuspended in PBS, and plasmids were isolated by Mini-prep
495 (Qiagen).

496 For genomic libraries, the identical procedure was performed, except 150mm petri plates
497 containing Cation-adjusted Miller-Hinton Broth containing 1ug/mL Trimethoprim and 1ug/mL
498 Chloramphenicol were used, plates were incubated for 2 days at 34degC, and plasmids were
499 isolated by Midi-prep (Qiagen). For the secondary screen in the folA* strain background,
500 Trimethoprim was used at 1mg/mL, necessitating 1% DMSO in the medium for solubility.

501

502 **Quantitative Screen for drug resistance**

503 Barcoded Synthetic mutant libraries prepared as above were diluted 1/1000 into 50mL of
504 LB medium containing 10ug/mL Chloramphenicol and 5ug/mL rifampicin. After growth
505 overnight at 34degC, a 5mL samples was taken, and this dilution was repeated for a second time
506 point. Samples of the initial plasmid library, the library when transformed into $\Delta mutS$, $\Delta recJ$,
507 $\Delta sbcB$ cells, and both timepoints, were obtained for plasmid purification.

508

509 **Deep Sequencing of Retron Donors**

510 *E. coli* containing retron plasmids were obtained from the relevant liquid or solid growth
511 condition, washed once with Dulbecco's Phosphate-buffered Saline, and their plasmids purified
512 via Miniprep or Midiprep (Qiagen). PCR amplification of retron donor sequences was performed
513 in a reaction containing 20uL q5 2x Mastermix (NEB), 2uL purified plasmid DNA, 0.4uL 50uM
514 primer mixture (Supplemental sequences), 1uL Evagreen dye (Biotium), and 15.6uL ddH2O.
515 Amplification was monitored in the SYBR channel on an Eppendorf Realplex4 real-time PCR
516 system until several cycles of productive amplification were observed, typically less than 10
517 cycles. Products were indexed for sequencing as described below.

518

519 **Amplicon sequencing**

520 Amplicons from previous steps were prepared for Illumina sequencing by first removing
521 oligonucleotides via treatment with Exonuclease I (NEB), then performing PCR using primers
522 adding Indexes 1 and 2 for Illumina Paired-end sequencing(Supplemental sequences). PCR was

523 performed in a reaction containing 10uL Q5 2X Mastermix (NEB), 1uL PCR product, .2uL
524 50uM primer mixture, 1uL Evagreen dye (Biotium), and 7.8uL ddH2O. Amplicons were purified
525 using DNA-binding beads³ and quantified using the Qubit dsDNA HS reagent (Thermo Fisher).
526 The resulting DNA were pooled and sequenced on MiSeq, NextSeq, or HiSeq Illumina
527 instruments, producing paired-end, 150bp reads.

528

529 **Sequence Analysis: Editing**

530 No fewer than 10,000 paired-end reads per replicate were merged using PEAR⁶ and
531 adapter and primer sequences trimmed using Cutadapt⁷. Sequences surrounding the edited region
532 were trimmed again with Cutadapt and counts of identical sequences were determined. Any
533 sequence occurring fewer than 20 times was assumed to be a rare sequencing error, and was
534 discarded at this stage. The edited fraction was calculated as the fraction of edited sequences
535 divided by the number of edited and wild type reference sequences detected within a sample. To
536 minimize the impact of sequencing error on conclusions, additional synonymous mutations were
537 incorporated along with the desired missense *gyrA* and *rpoB* alleles for Figure 1B, where edited
538 events are often rare. This more unambiguously links an edited sequence to an editing event, and
539 not to mutation or errors during PCR/sequencing. A subset of these genotypes were additionally
540 replicated by a phenotypic test- the efficiency of plating on antibiotic(Fig S1C). The fraction of
541 all observed sequences which were either edited or wild type was monitored, and exceeded 93%
542 for the results in Figure 2B and exceeded 99% for the additional alleles in Figure 2D. Scripts are
543 available at <https://github.com/churchlab/rlr>.

544

545 **Culture-based confirmation of editing results**

546 In parallel with amplicon sequencing to measure editing, serial dilutions of samples
547 bearing the *RpoB* donor were plated to LB with 25ug/mL Chloramphenicol, and LB with 25ug
548 Rifampicin. CFU/mL was determined by counting colonies, and the proportion of Rifampicin
549 resistant CFU was used as a proxy for the edited fraction of cells.

550

551 **Sequence Analysis: Synthetic DNA experiments**

552 Paired-end reads were merged using PEAR⁶, adapter and primer sequences were trimmed
553 off using Cutadapt⁷, and counts of identical sequences were determined. Donor sequences not

554 matching expected sequences were discarded. The fraction of sequences discarded correlated
555 with estimated sequencing error rate and quality scores, and was never $\geq 25\%$ of sequences. The
556 frequency of each donor in the resulting dataset is then determined. For timecourses, these
557 frequencies are normalized to the median frequency of the neutral allele retrон pool within each
558 replicate and time point, and initialized to their relative frequency in the first time point prior to
559 plotting. For calculating relative growth rates, an exponential curve was fit to non-initialized
560 trajectories using a linear model. Scripts are available at <https://github.com/churchlab/r lr>.

561

562 **Sequence Analysis: Natural DNA experiments**

563 For determining the length of retron donor regions in cloned gDNA libraries, reads were
564 first aligned to the MG1655 reference genome using BWA-MEM⁸. The length of the region
565 between aligned read pairs, the Template Length or Tlen column, was extracted from this
566 alignment and visualized as a histogram(Fig S6A). Template lengths longer than 500 base pairs
567 were assumed to be the result of erroneous alignment, and were discarded.

568 For other analyses paired-end reads were merged using PEAR⁶ and adapter and primer
569 sequences trimmed off using Cutadapt⁷. The resulting sequences were aligned to the MG1655
570 reference genome using BWA-MEM⁸. To determine coverage of the reference genome, depth
571 was determined using Bedtools genomecov⁹, and visualized by plotting the mean coverage of
572 1000bp sliding windows(Fig 4B). Alternatively, to examine non-redundant coverage conferred
573 by unique donors, sequences with identical start and end alignment positions were collapsed into
574 a single sequence before determining depth, visualized by plotting the mean coverage of 500bp
575 windows(Fig S6B). When examining a subset of the genome, coverage at every base was used,
576 rather than using sliding windows (Fig 4C).

577 To determine the abundance of retron donors conferring SNPs, reads from amplicons
578 obtained after selection were aligned to the MG1655 reference genome and SNPs inferred using
579 Millstone¹⁰. Depth of SNP coverage in the resulting output reflects abundance in the pool, and
580 was used for visualization and analysis.

581

582 **Individual Growth rate measurements**

583 Colonies were picked into 100uL of LB medium in 96 well plates and grown for 4-6
584 hours at 34 degrees. 10uL of a 10-fold dilution of this “pre-culture” was used to innoculate

585 190uL of LB medium with relevant additives in a Nunclon 96-well microwell plate (Thermo
586 Scientific). These plates were cultured in a shaking plate reader at 34 degrees, measuring OD₆₀₀
587 every 15 minutes. The resulting data were analyzed using the analyze_growth.m script to derive
588 growth rates for all wells. Scripts are available at <https://github.com/churchlab/rLR>.

589

590 Population genetics model

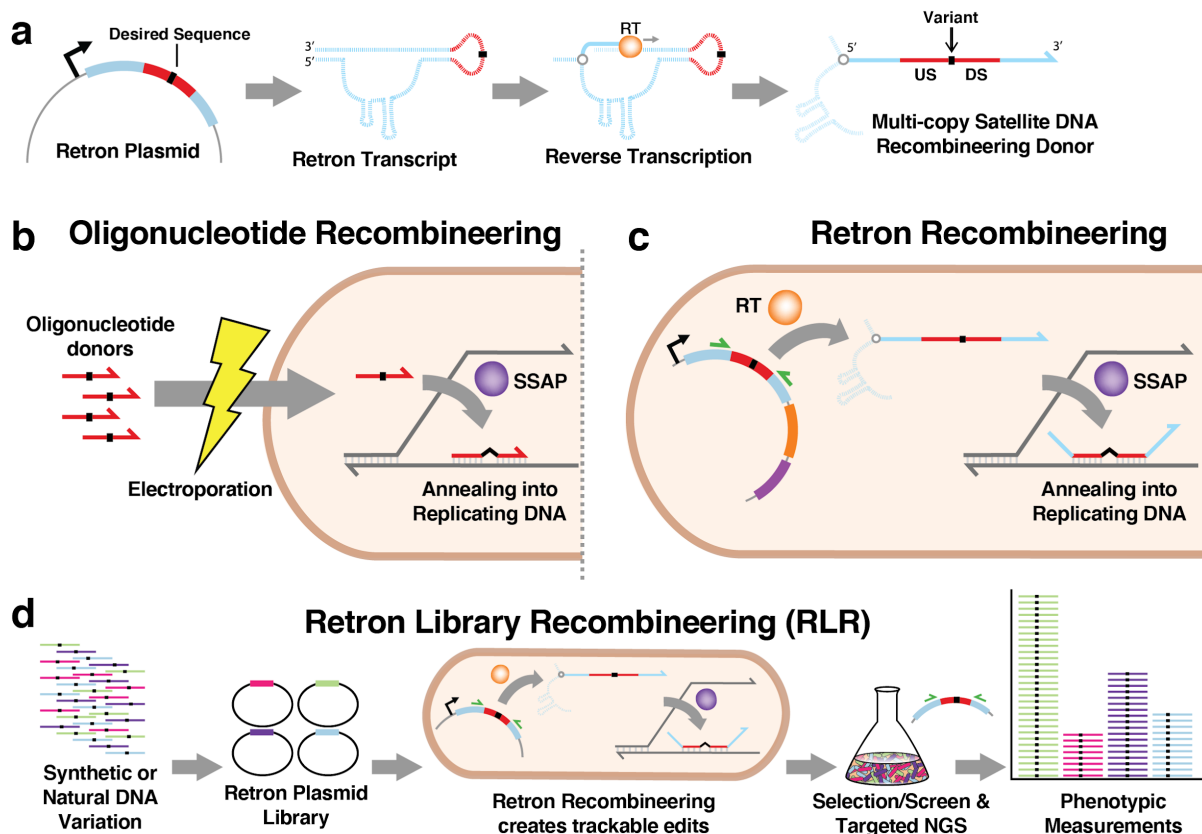
591 A simulation was written in the Matlab scripting language, in which each generation, a
592 fraction 'r' of un-edited cells become edited, for a population bearing a particular retron. Once
593 edited, that population reproduces at a rate of 'f', which may be more or less than the parental
594 rate of 1. Simulations can be performed with various r and f and initial conditions. The model
595 makes implicit assumptions that populations experience constant, uniform exponential growth
596 and never approach carrying capacity of their environment. Scripts are available at
597 <https://github.com/churchlab/rLR>.

598

599 Online Methods References:

- 600 1. Datsenko, K. A. & Wanner, B. L. One-step inactivation of chromosomal genes in
601 Escherichia coli K-12 using PCR products. *Proc. Natl. Acad. Sci. U. S. A.* **97**, 6640–6645
602 (2000).
- 603 2. Wong, B. G., Mancuso, C. P., Kiriakov, S., Bashor, C. J. & Khalil, A. S. Precise, automated
604 control of conditions for high-throughput growth of yeast and bacteria with eVOLVER. *Nat.*
605 *Biotechnol.* **36**, 614–623 (2018).
- 606 3. Oberacker, P. *et al.* Bio-On-Magnetic-Beads (BOMB): Open platform for high-throughput
607 nucleic acid extraction and manipulation. *PLOS Biology* vol. 17 e3000107 (2019).
- 608 4. Bonde, M. T. *et al.* MODEST: a web-based design tool for oligonucleotide-mediated
609 genome engineering and recombineering. *Nucleic Acids Res.* **42**, W408–15 (2014).
- 610 5. Tian, S. & Das, R. Primerize-2D: automated primer design for RNA multidimensional
611 chemical mapping. *Bioinformatics* **33**, 1405–1406 (2017).
- 612 6. Zhang, J., Kobert, K., Flouri, T. & Stamatakis, A. PEAR: a fast and accurate Illumina
613 Paired-End reAd mergeR. *Bioinformatics* **30**, 614–620 (2014).
- 614 7. Martin, M. Cutadapt removes adapter sequences from high-throughput sequencing reads.
615 *EMBnet.journal* vol. 17 10 (2011).
- 616 8. Li, H. Aligning sequence reads, clone sequences and assembly contigs with BWA-MEM.
617 *arxiv.org* (2013).
- 618 9. Quinlan, A. R. & Hall, I. M. BEDTools: a flexible suite of utilities for comparing genomic
619 features. *Bioinformatics* **26**, 841–842 (2010).
- 620 10. Goodman, D. B. *et al.* Millstone: software for multiplex microbial genome analysis and
621 engineering. *Genome Biol.* **18**, 101 (2017).

Figure 1



622

623 **Figure 1: Graphical Introduction to Retron Library Recombineering**

624 **1A** A retron contains a region msr/msd which undergoes targeted reverse-
625 transcription, catalyzed by a retron reverse transcriptase (RT), producing multi-copy
626 satellite DNA. A novel sequence (red) introduced into retron becomes part of the
627 reverse-transcribed product. When this sequence contains homology upstream (US)
628 and downstream (DS) of a sequence alteration (black), multi-copy satellite DNA can be
629 used as a single-stranded recombineering donor. RNA is depicted with dashed lines,
630 whereas DNA is depicted with solid lines.

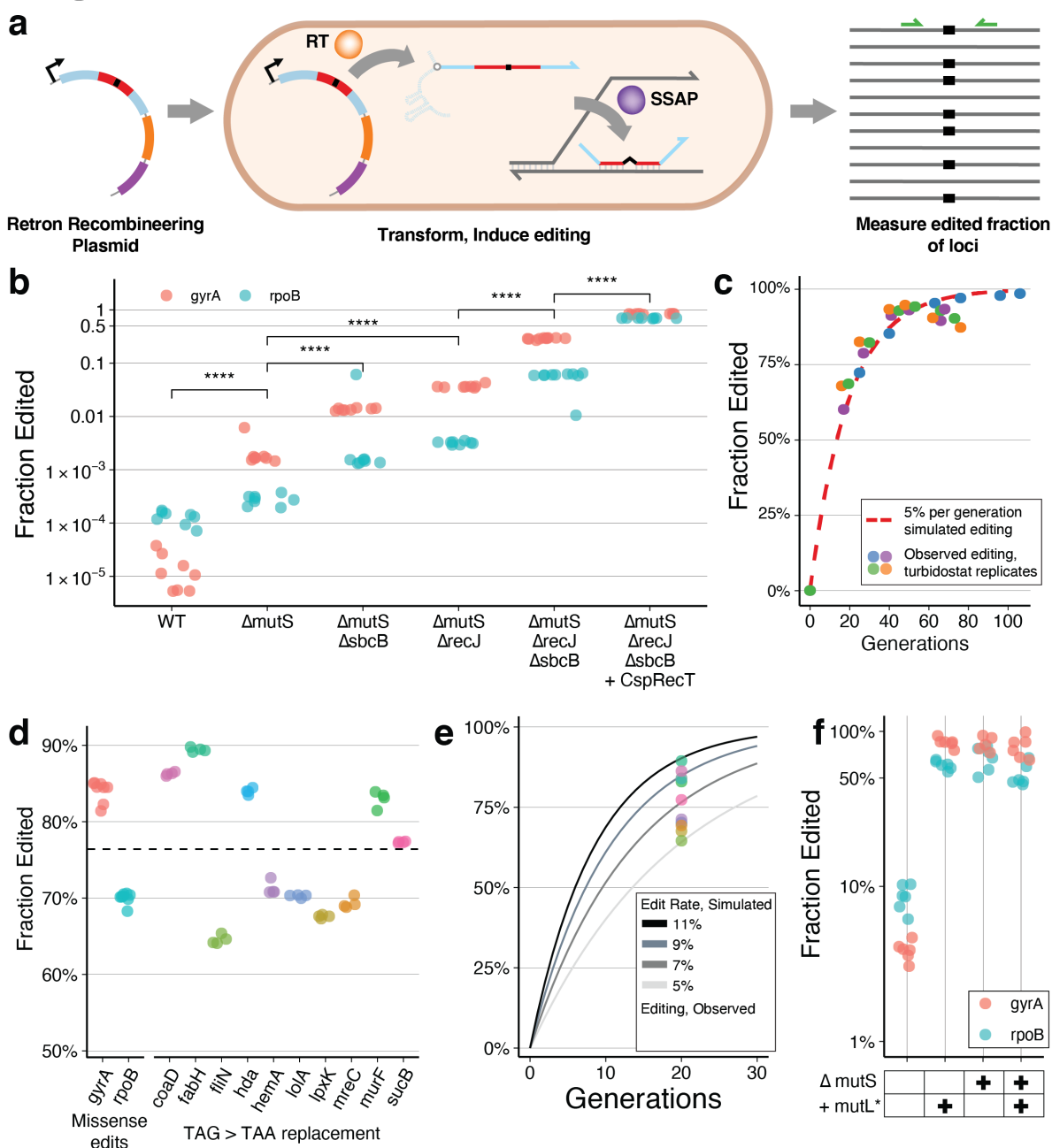
631 **1B** Oligonucleotide recombineering is a technique in which synthetic oligonucleotide
632 donors are introduced into bacteria and anneal to replicating DNA. This process is
633 catalyzed by a Single-Stranded Annealing Protein (SSAP), and results in desired
634 sequence alterations (black) being incorporated into the genome.

635 **1C** Retron Recombineering is similar to oligonucleotide recombineering, but uses
636 multi-copy satellite DNA produced by a retron as donor DNA, rather than transformed

637 oligonucleotides. An SSAP is required for annealing of the donor, and retron Reverse
638 Transcriptase (RT) is additionally required to create the donor. The retron plasmid
639 remains in the cell, where it is available for targeted amplicon sequencing using
640 complementary primers (green).

641 **1D** Retron Library Recombineering (RLR) is a pooled functional genomics technique.
642 Synthetic or natural DNA containing variation is used to construct a library of retron
643 plasmids. Cells transformed with a given retron plasmid incorporate the variation within
644 a retron donor, and the plasmids remain within cells as “barcodes” to distinguish mutant
645 lineages. Next generation sequencing (NGS) of amplicons created using
646 complementary primers (green) before and after a selection or screen reveals the
647 abundance, and therefore the phenotypes, of individual variants.

Figure 2



648 **Figure 2: Editing the Genome using Retrons**

649 **2A** Experiment measuring the edited fraction obtained for a desired mutation. A
 650 retron plasmid creates multi-copy single stranded DNA via a retron Reverse
 651 Transcriptase (RT). This DNA is incorporated into the genome via a co-expressed
 652 single stranded annealing protein (SSAP) as in Figure 1C. The edited fraction of
 653 resulting genomes is observed by amplicon Next Generation Sequencing (NGS),

654 facilitated by primers targeting the locus (green).

655 **2B** The effect of genotype on the edited fraction of loci, measured after induction of
656 retron system and batch growth for approximately 20 generations. Colors differentiate
657 experiments incorporating mutations at the *gyrA* and *rpoB* loci. Individual replicates are
658 indicated with dots. “****” indicates $p < 0.0001$ resulting from a two-sided, unpaired
659 parameteric t-test performed between genotype groups indicated with brackets.

660 **2C** $\Delta mutS \Delta sbcB \Delta recJ$ cells were transformed with the *gyrA*-editing retron plasmid
661 expressing Beta as an SSAP. Transformed cells were grown and induced continuously
662 in 4 replicate turbidostats for 73 hours, sampling over time. The number of generations
663 experienced by a given timepoint was inferred from the turbidostat growth record, and the
664 edited fraction was determined by *gyrA* amplicon NGS for each sample. These data are
665 shown alongside a simulated editing trajectory of an allele with neutral fitness effect,
666 editing at 5% per generation.

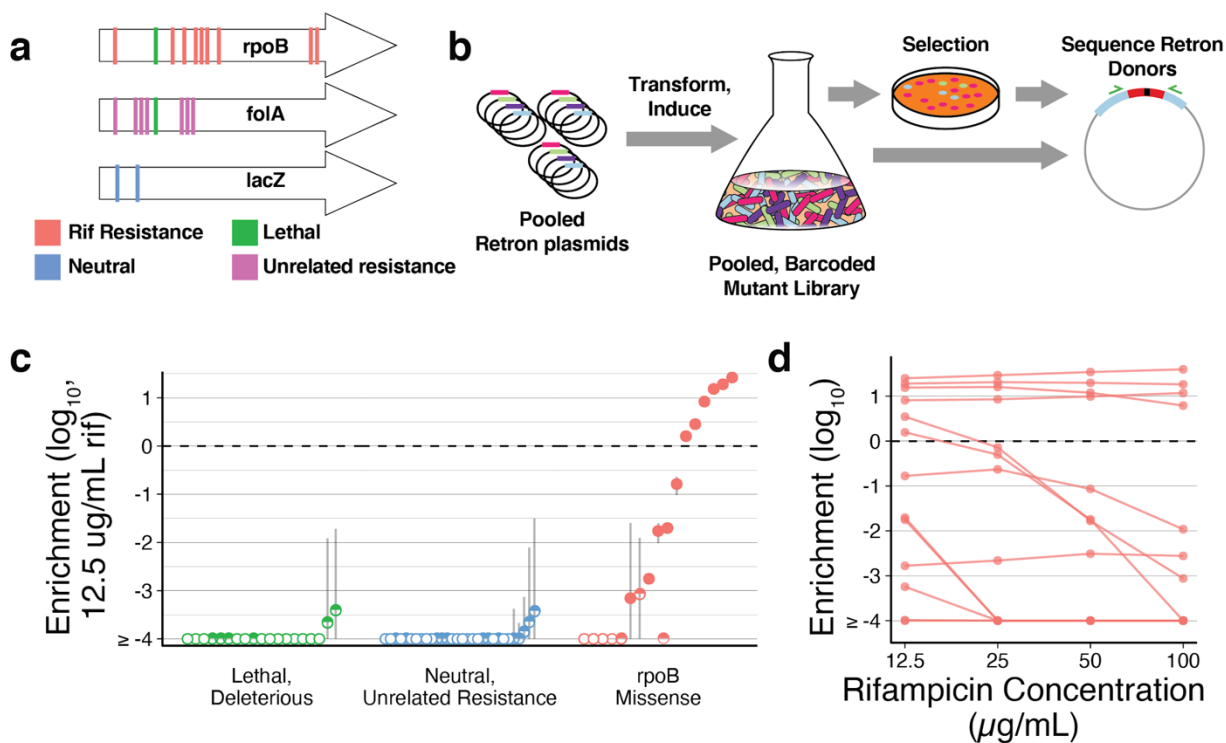
667 **2D** Edited fraction observed across alleles, after approximately 20 generations of
668 induction and batch growth. A retron plasmid containing CspRecT as an SSAP was
669 expressed in the $\Delta mutS \Delta recJ \Delta sbcB$ background in all cases. Results of individual
670 replicates are shown as dots. Results for *gyrA* and *rpoB* missense alleles (Fig 2B) are
671 shown again for comparison alongside TAG>TAA stop codon editing for 10 essential
672 genes. The mean edited fraction achieved across the 12 loci, 76.4%, is indicated by
673 dashed line.

674 **2E** Mean edited fraction of the loci in Figure 2D are shown alongside a simulated
675 editing trajectory of alleles with neutral fitness effect. This provides estimates of editing
676 rates across alleles as within the range of 5-11% per generation.

677 **2F** Retron plasmids with and without a dominant-negative MutL-E32K variant
678 (*mutL*^{*})²¹ were expressed in batch growth, in strains with and without inactivation of
679 *mutS* ($\Delta mutS$). Retron plasmids targeted the *gyrA* and *rpoB* loci and used CspRecT as
680 an SSAP. Four replicate experiments per locus and condition are indicated with dots.

681

Figure 3



682 **Figure 3: Pooled measurement of phenotypes using RLR**

683 **3A** Example alleles contained in a synthetic pool. Both known and suspected
684 rifampicin resistance alleles were specified in the pool, as well as resistance alleles for
685 unrelated drugs, and control alleles expected to be neutral, lethal, or deleterious. For
686 more details on edits specified, see Online Methods and Supplemental Table 2.

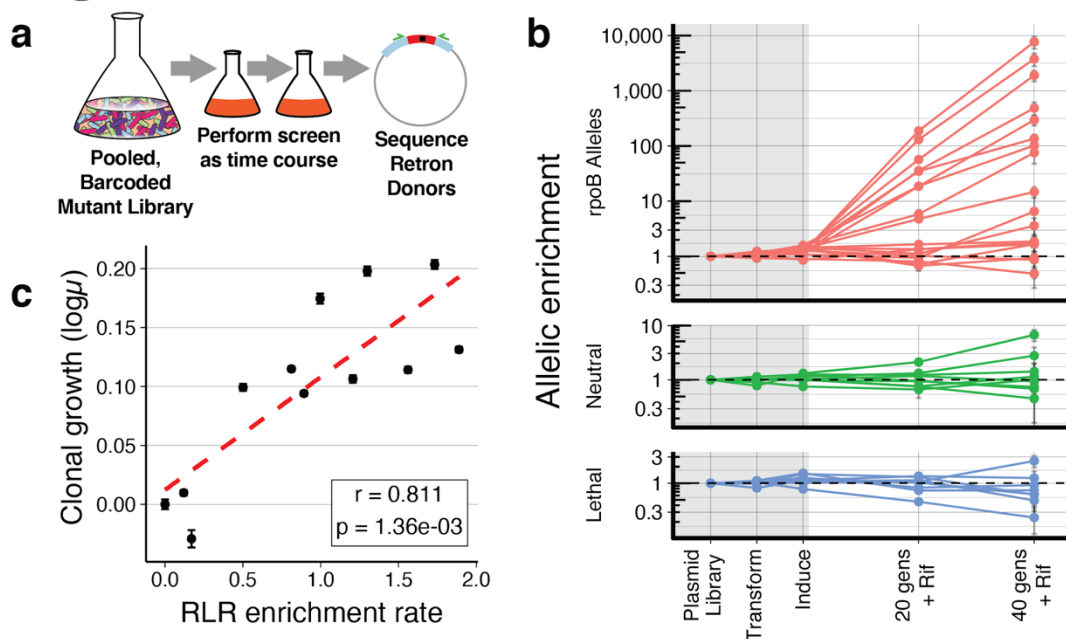
687 **3B** Graphical representation of an RLR experiment to identify antibiotic resistance
688 alleles. A pool of Retron plasmids conferring alleles of interest are transformed into
689 cells. These transformants are induced, resulting in a pooled, barcoded mutant library.
690 The library is subjected to selection, and the frequencies of retron donors are compared
691 before and after treatment to calculate a resistance phenotype for each allele.

692 **3C** RLR enrichment values of alleles, observed in a rifampicin treatment experiment.
693 The median of three replicate experiments is indicated with a dot, and error bars are the
694 Standard Error of the mean. A pseudocount of one is given to any allele not detected by
695 sequencing after treatment, such that frequencies reported are a lower limit of detection
696 in these cases. Unfilled points indicate when an allele was not detected among any of
697 the three replicates after rifampicin treatment, and a half-filled point indicates when an

698 allele was only detected in a subset of replicates. An enrichment value of zero is
699 marked with a horizontal dashed line, indicating identical relative abundance before and
700 after rifampicin treatment.

701 **3D** For *rpoB* missense alleles, allelic enrichment across concentration of rifampicin is
702 displayed. The median of three independent experiments is indicated with a dot, and
703 lines connect an allele across concentrations.

Figure 4



704 **Figure 4: Quantitative measurement of phenotypes using RLR**

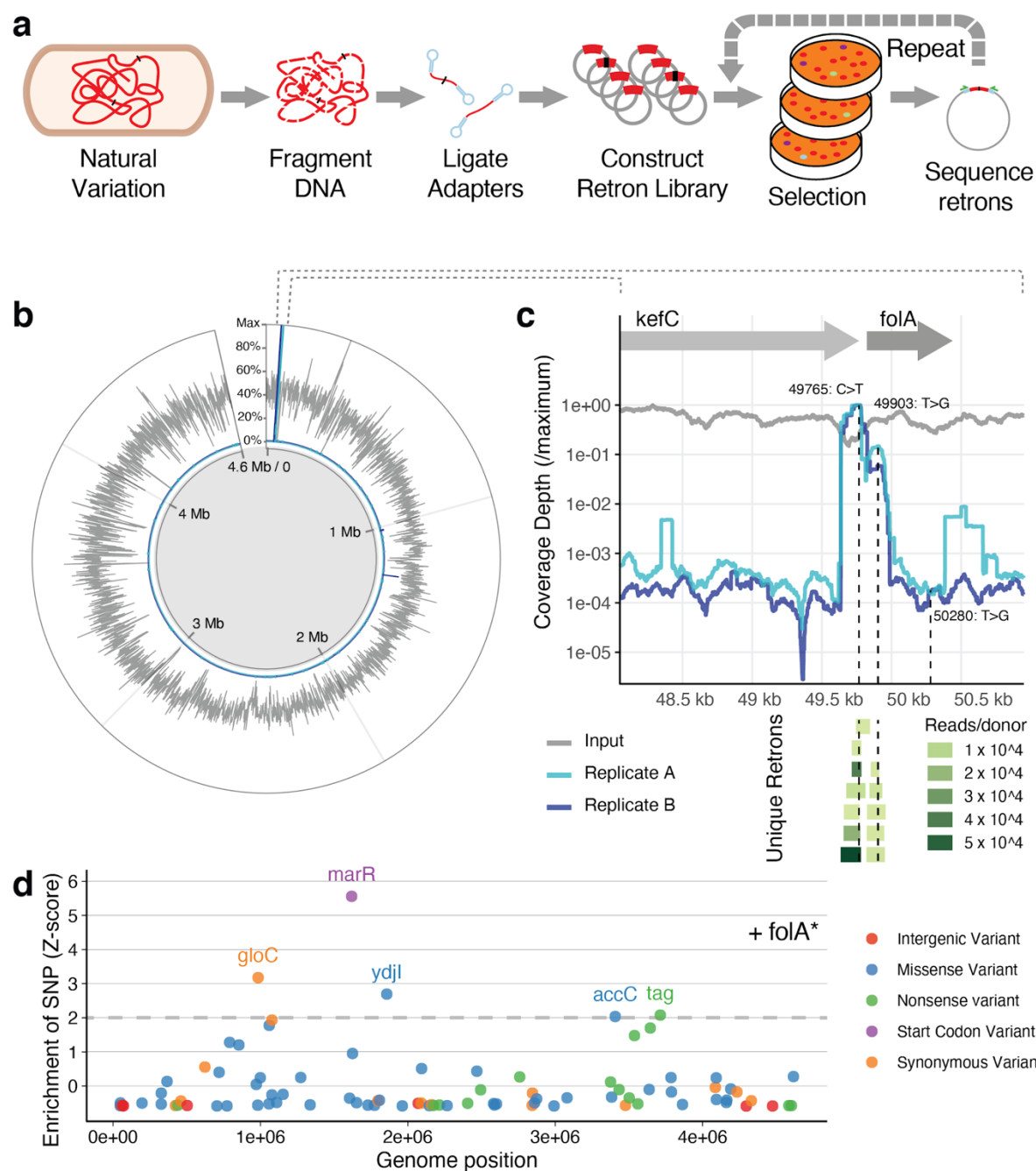
705 **4A** Graphical representation of a quantitative RLR experiment. A pooled, barcoded
706 mutant library constructed via RLR is subjected to a treatment time course, and the
707 relative abundance of retron donors are measured over time.

708 **4B** Frequencies of retron plasmids measured by targeted Next Generation
709 Sequencing during an experiment are shown. Frequencies of each allele are normalized
710 to the median of neutral controls within each timepoint, and to their starting abundance
711 in the plasmid pool, for clarity. Frequency measurements within the grey rectangle occur
712 during construction, transformation, and induction of the retron library. Measurements in
713 the white area occur during growth in sub-inhibitory rifampicin, 5ug/mL. The mean
714 across three replicates is indicated with a dot, and error bars are the Standard Error of
715 this mean. Horizontal dashed lines indicate an allelic enrichment of 1, no change in
716 frequency.

717 **4C** A measure of growth rate for all alleles in the experiment can be determined by
718 fitting an exponential curve to normalized frequency during the experiment, and
719 reporting the the slope of normalized \log_{10} allelic enrichment, over time. For a sample
720 of 11 resistance mutants, the mean RLR slope across 3 replicate experiments is plotted
721 on the X axis, and \log_{10} of growth rates measured individually using classical methods

722 are plotted on the y-axis. r is Pearson's correlation coefficient between these two
723 measures, and the p-value is the probability of these results given the null hypothesis of
724 no correlation. Wild-type growth inferred from Neutral controls is plotted as an additional
725 point. Error bars depict the standard error of clonal growth measurements, data
726 visualized in Figure S4A

Figure 5



727 **Figure 5: Detecting causal variants in genomic DNA using retroviral libraries**
728 **5A** Graphical summary of an RLR experiment with genomic DNA (gDNA) as a
729 source of alleles. gDNA of an evolved strain is randomly fragmented, and identical
730 adaptors ligated to the ends of these fragments. These adaptors allow pooled cloning,

731 creating a library of retron plasmids having millions of members. This library is induced,
732 a selection is conducted, and retron donors of surviving mutants are sequenced as a
733 pool via amplicon NGS. Optionally, mutants surviving selection can be transformed by
734 the pool again, screening for additional mutations and combinatorial effects.

735 **5B** Results of genomic DNA screen. Coverage of unique donor sequences across all
736 genomic positions is displayed for a Genomic Retron Library, showing the mean
737 coverage across 1000 base-pair windows and normalizing to the maximum coverage
738 observed (Gray, see Supplementary figure 6B for additional detail). After selection, the
739 depth at which variants are observed in surviving retron donors is depicted for two
740 replicates of retron induction and selection on Trimethoprim, normalized to the
741 maximum depth observed at a genomic position(blue, light blue).

742 **5C** The region surrounding the *folA* locus is displayed, with genomic position on the
743 X axis. Sequence coverage observed for each base is plotted on the Y axis for the input
744 genomic retron library and for two replicates post-selection, relative to the maximum
745 coverage observed in this region for a given sample. Below, retron donor sequences
746 observed more than 1000 times in replicate A are depicted as a “pileup” aligned to the
747 genome, and are colored by their abundance in post-selection sequencing. SNPs
748 detected at the *folA* locus are indicated by vertical dashed lines, highlighting enrichment
749 of two SNPs, and lack of enrichment of a third.

750 **5D** Transforming the library into a strain already bearing these detected *folA*
751 mutations (*folA**) and plating on additional Trimethoprim exposes additional candidate
752 causal variants. Retron donors sequenced post-selection are used to calculate Z-scores
753 for each allele, describing their deviation from mean allele depth of coverage. Variants
754 with Z-scores over 2 have been labeled by the gene in which they occur, and variants
755 have been classified by their relationship to coding sequences.